Eur. Phys. J. Plus (2020) 135:375
https://doi.org/10.1140/epjp/s13360-020-00375-y

THE EUROPEAN PHYSICAL JOURNAL PLUS

Regular Article

Reconciling the observed mid-depth exponential ocean stratification with weak interior mixing and Southern Ocean dynamics via boundary-intensified mixing

Madeline D. Miller[1,2,a], **Xiaoting Yang**[1], **Eli Tziperman**[1]

[1] Department of Earth and Planetary Sciences and School of Engineering and Applied Sciences, Harvard University, Cambridge, MA, USA
[2] Present Address: MIT Lincoln Laboratory, Lexington, MA, USA

Received: 12 January 2020 / Accepted: 1 April 2020 / Published online: 27 April 2020

Abstract Munk (Deep Sea Res Oceanogr Abstr 13(4):707–730, 1966) showed that the mid-depth (1–3 km) vertical temperature profile is consistent with a one-dimensional vertical advection–diffusion balance, with a constant upwelling and an interior diapycnal diffusivity of $\mathcal{O}(10^{-4})$ m^2 s^{-1}. However, typical observed diffusivities in the interior are $\mathcal{O}(10^{-5})$ m^2 s^{-1}. Recent work suggested that the mid-depth stratification is set by Southern Ocean (SO) isopycnal slopes, governed by SO wind and eddies, that communicate the surface outcrop positions to the mid-depth ocean. It is shown here, using an idealized ocean general circulation model, that while SO dynamics play an important role by linking the surface water mass transformation by air-sea fluxes with the mid-depth interior stratification, they do not set the observed *exponential* stratification and that interior mixing must contribute. Strong diapycnal mixing concentrated near the ocean boundaries is shown to be balanced locally by upwelling. A one-dimensional Munk-like balance in these boundary-mixing areas, although with much larger mixing and upwelling, leads to an exponential mid-depth temperature stratification, which spreads via isopycnal advection and mixing to the ocean interior. The exponential profile is robust to vertical variations in the vertical velocity and persists despite the observed weak interior diapycnal mixing. These results may suggest a way to reconcile the observed exponential interior mid-depth temperature stratification, the weak diapycnal diffusivity observed in tracer release experiments, and the role of Southern Ocean dynamics.

1 Introduction

The observed mid-depth (defined here as 1–3 km depth) ocean interior vertical potential density profile and its derivative can both be fit to very good accuracy by an exponential function in many ocean regions, as shown by the four examples of Fig. 1. As noted by Munk [19], an exponential temperature profile is also the solution to the one-dimensional vertical advective–diffusive balance, $w\partial T/\partial z = \kappa_v \partial^2 T/\partial z^2$ with a constant diffusive mixing coefficient $\kappa_v = 10^{-4}$ m^2 s^{-1} and a constant upwelling w such that $\kappa_v/w \sim 1$ km. While global water mass budget calculations are consistent with such mixing values [10], direct measurements of κ_v in the ocean interior based on turbulent dissipation measurements and tracer

[a] e-mail: madeline.miller@ll.mit.edu (corresponding author)

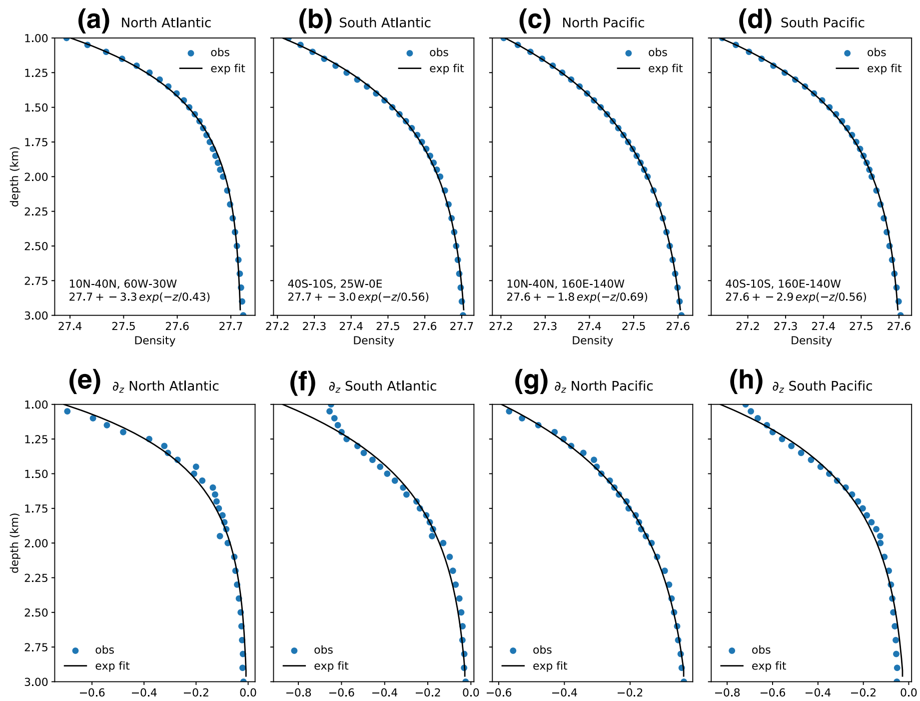

Fig. 1 The observed interior mid-depth potential density and corresponding exponential fits, for the North and South Atlantic and Pacific oceans (upper panels), and the vertical derivatives of the potential density (lower panels, multiplied by 1000)

release experiments suggest ocean interior vertical mixing values that are ten times smaller, $\mathcal{O}(10^{-5})$ m^2 s^{-1} [9,23], leaving the cause of the exponential stratification unexplained.

The mid-depth ocean stratification received significant attention over the past decade, and recent studies have focused on two alternative explanations. First, that ocean mixing is enhanced near horizontal ocean boundaries, where the stratification is set, so that the Munk diffusivity holds as an *averaged* mixing rate. Second, that the stratification is set in the Southern Ocean (SO) by the effect of wind and eddies, rather than by the mid-depth vertical interior mixing. We now review these studies, noting that they mostly focused on what sets *a* mid-depth stratification rather than on what sets the robustly observed *exponential* stratification.

In the first group of studies, Samelson [26], while not addressing the exponential shape of the mid-depth stratification profile, used a general circulation ocean model (GCM) with enhanced vertical mixing near horizontal boundaries to explain the discrepancy between the existence of a large-scale mid-depth stratification and the weak observed vertical mixing. Marotzke [12] and Scott and Marotzke [27] demonstrated the effects of such boundary mixing in a GCM on the overturning circulation. The first paper assumed an exponential stratification in the shown theory but did not address its cause while the second paper shows (their Fig. 11) a non-exponential stratification. Munk [19] already suggested a significant role for strong mixing along the ocean boundaries, allowing for the possibility that $\kappa_v = 10^{-4}$ m^2 s^{-1} represents an averaged effective mixing (as did some more recent works, e.g., [21,28]). In a follow-up on the abyssal recipes paper, Munk and Wunsch [18] attempted to fit exponential profiles to the observed stratification and used a toy model to show that exponential stratification can result from strong boundary vertical mixing together with effective horizontal advection. However, their prescribed vertical velocity is assumed constant throughout the domain and the toy model represents an advection–diffusion equation only and does not include any dynamics. We show here that strong boundary mixing is likely accompanied by strong localized vertical boundary advection as well.

In the second group of studies, Vallis [35] and Henning and Vallis [5] studied the effects of a SO channel geometry and SO eddies, in a single-hemispheric GCM configuration, on the existence of a mid-depth stratification, yet without discussing its exponential form. Wolfe and Cessi [38] continued this line of study and showed that without a SO channel there is no mid-depth stratification in the interior of the ocean. They suggested that the stratification in the presence of a SO, in the adiabatic limit, should be independent of the value of κ_v, although the stratification they calculated is non-exponential (their Figs. 6 and 8). Wolfe and Cessi [39] further showed that a residual overturning circulation requires isopycnals that outcrop both in the north and south and a SO channel, but again did not discuss the exponential structure of the mid-depth stratification. Nikurashin and Vallis [21] used both a theoretical model based on a Transformed Eulerian Mean formulation and a GCM to show that wind, eddies and the channel configuration of the SO, as well as interior mixing, are all needed to get a mid-depth stratification. Nikurashin and Vallis [22] added a northern source of deep water and reinforced the conclusions of their 2011 work, but both works did not discuss the source of the exponential stratification, and the stratification shown (Fig. 10 in the 2012 paper) is non-exponential. Furthermore, they state, for example, “In the limit of weak diapycnal mixing, typical for the mid-depth ocean, deep stratification throughout the ocean is produced by the effects of wind and eddies in a circumpolar channel and maintained even in the limit of vanishing diapycnal diffusivity and in a flat-bottomed ocean.” A strong-mixing case (2012 paper, sect. 4a2) that can, in principle, lead to exponential stratification is considered by the authors to be irrelevant for the present-day mid-depth stratification due to the weak mixing observations. The role of SO eddies and the adiabatic overturning circulation are nicely summarized in the review by Johnson et al. [7]. We show here that the presence of a SO by itself is not sufficient to obtain an observed-like *exponential* interior stratification, without the effects of boundary mixing.

In some related works studying SO eddy dynamics, that served as a background for the above work trying to understand the role of the SO in setting the interior stratification, Marshall and Radko [15] and Ito and Marshall [6] prescribed the vertical stratification of the interior north of the SO and therefore did not attempt to explain the interior stratification away from the SO. Shakespeare and McC. Hogg [28] also studied the response of the ocean to SO winds and prescribed surface buoyancy fluxes, yet their 3-layer formulation did not allow them to examine the mid-depth exponential stratification profile.

The Munk paradigm for the exponential stratification poses another challenge in addition to the conflict with the weakness of observed mixing rates. It assumes that the diffusivity and upwelling are constant in depth, while both are expected to vary vertically within the interior water column. This was addressed by Tziperman [34] who suggested that the interior stratification is set by a balance between the net water mass formation near the surface into a given range of isopycnals, and the cross-isopycnal fluxes due to interior mixing, which depends on the interior stratification. The two processes must maintain a constant time-mean total mass between any two isopycnals. If the surface formation and interior mixing effects do not balance, the outcrop position and resulting air sea fluxes, as well as the mid-depth stratification, will adjust until such a balance is obtained. Tziperman [34] further showed that a Munk-like vertical balance produces a very-nearly exponential temperature stratification even when the upwelling and diffusivity are not constant in the vertical (z) direction and applied these ideas to calculate the basic stratification prescribed on the eastern boundary in adiabatic thermocline theories [11,25].

It should be clear from the above discussion that the mechanism that sets the exponential mid-depth stratification is not well understood. Boundary mixing has been suggested to play a role, but no explicit demonstration of how it would affect the stratification in a full dynamical model has been provided. SO eddies have clearly been shown to help establish a mid-depth stratification, but the resulting stratification is not necessarily exponential in the nearly adiabatic limit corresponding to the observed interior mixing rates. And finally, the Munk picture is based on an unrealistic assumption of vertically uniform upwelling and mixing rates. These issues are the focus of the present work.

We focus on the *exponential* mid-depth stratification. We examine the connections between the primary processes that have been proposed: interior diapycnal mixing, boundary mixing, and SO eddy dynamics and isopycnal slopes. We show that enhanced diapycnal mixing near horizontal boundaries can lead to an exponential profile equivalent to the Munk picture even when the interior diapycnal mixing is very weak. We also show that while this occurs via a Munk-like balance within the enhanced mixing boundary regions, it involves much stronger upwelling and mixing rates in these regions than in the original Munk picture, unlike the role of boundary mixing envisioned, for example, in the toy model of Munk and Wunsch [18]. We further show that the exponential profile is not sensitive to vertical variations in the magnitude of the upwelling. SO eddy dynamics and isopycnal slopes do play a critical role in communicating between the surface and deep water mass transformation processes, but do not set the *exponential* interior stratification away from the SO. In order to focus only on the relevant factors, we employ idealized GCM experiments in a basin-channel configuration of an ocean model similar to Wolfe and Cessi [38]. We prescribe enhanced vertical mixing near horizontal ocean boundaries, similar to Marotzke [12] and Samelson [26], but we additionally include a SO-like channel which they have not and discuss the exponential stratification which was not addressed by these studies.

The idea of stronger boundary mixing motivating this study is supported by observational evidence, theory and modeling, which all indicate elevated diapycnal diffusivity near rough topography, ocean boundaries and ocean passages (e.g., [17,20,23,23,29,31–33,37]). While observations of mixing rates and turbulent diffusivity are sparse, they do indicate significant diapycnal mixing may be found at the ocean margins.

The mid-depth ocean stratification deviates from exponential in some regions, while in others the density is very nearly exponential although the temperature is not (e.g., within the South Atlantic ocean north of the Southern Ocean). While a more thorough quantification of where the stratification is exponential is outside the scope of this study, the examples shown in Fig. 1 are sufficiently intriguing and representative of large areas that they justify the discussion attempted here. The exponential depth scales shown in Fig. 1 are generally less than the canonical 1 km value calculated by Munk. It is difficult to directly deduce a vertical mixing estimate from this scale, as that scale also depends on the strength of upwelling. Our objective is to form a consistent *qualitative* picture that reconciles the exponential stratification with very weak ocean interior mixing. We leave it to future studies to examine the difference between different ocean basins and to re-evaluate Munk's recipes based on updated values for both the upwelling and diffusivities. The approach taken here is highly idealized; we do not address the fact that deep isopycnals outcrop both in the SO and the North Atlantic [38]; our domain is idealized; eddies are not resolved; the effects of salinity are ignored; the specified boundary mixing is crude; we did not include the potentially important effects of sloping boundaries Ferrari et al. [3]; we do not include the effect of vertical variations in the vertical mixing coefficient that is known to also affect the deep stratification Mashayek et al. [16]; and more.

In the following sections, we introduce the model, the numerical experiments, and some analysis methods (Sect. 2); show and analyze the main results of the numerical experiments (Sect. 3); demonstrate that in the presence of interior diapycnal mixing (whether boundary or interior); the stratification profile tends to be robustly exponential even if the upwelling velocity is not uniform in depth (Sect. 4); and conclude in Sect. 5.

2 Ocean model and experiments

We show results from three numerical experiments in an idealized ocean basin with an Antarctic Circumpolar Current (ACC) channel. Our experimental design combines experiments similar to those of Samelson [26] with a configuration that contains a SO-like channel similar to Wolfe and Cessi [38]. We use the Massachusetts Institute of Technology generalized circulation model (MITgcm) hydrostatic ocean model [13]. The domain is a 3500-m-deep, flat-bottomed rectangular box spanning 60° in longitude and 140° in latitude (70°S to 70°N) at a 1° horizontal resolution. In the Southern Hemisphere, there is a zonally re-entrant channel that spans 70°S to 50°S. There are 45 vertical levels ranging from a thickness of 10 m in the surface layer to 261.5 m in the lowest layer. The model equations are solved on a spherical polar grid. Sub-gridscale mixing is parameterized with Gent-McWilliams/Redi isopycnal mixing [4,24] and a K-Profile Parameterization of vertical mixing [8]. Background Laplacian and biharmonic horizontal viscosities are $10^6\,m^2\,s^{-1}$ and $10^{10}\,m^4\,s^{-1}$ for eliminating grid-scale noise. Background vertical viscosity is set to $10^{-3}\,m^2\,s^{-1}$. The salinity is set to a uniform value, and the equation of state is linear in temperature with $\rho_0 = 1028.665\,kg\,m^{-3}$, $T_0 = 20\,°C$ and $\alpha = 1665.22 \times 10^{-7}\,kg\,m^{-3}\,°C^{-1}$.

The surface forcing, shown in Fig. 2 is modeled after Wolfe and Cessi [38] to be both idealized and generically representative of modern meridional asymmetry in surface wind and temperature fields in the Pacific Ocean. The zonal surface wind is zonally symmetric and the wind maximum over the re-entrant channel is $0.2\,N\,m^{-2}$, twice the maximum of $0.1\,N\,m^{-2}$ in the Northern Hemisphere. There are also two relative minima in wind stress of $-0.07\,N\,m^{-2}$ bounding the equator. There is no meridional wind forcing. Temperature in the surface layer is relaxed towards a zonally symmetric temperature field on a 1-week timescale to the values shown in Fig. 2b. As in the observed Pacific Ocean, the restoring surface temperature in the Southern Hemisphere is colder than the surface temperature in the Northern Hemisphere. We accelerate the model experiments to steady state using asynchronous time-stepping [2] with deltaTmom = 300 s and deltaTtracer = 3000 s for 3500 model years. We then confirm the model is at steady state by running it for 100 years with synchronous time-steps (deltaTmom = deltaTtracer = 300 s) and take the steady-state values as when the trends of SST, temperature and KE are less than 1% of their respective 20-year mean values. All steady-state quantities are averaged over a 10-year time interval integrated with synchronous time steps. However, the integrations approach a steady state, as the model is of a coarse resolution and shows no variability at steady state.

The experiment termed MinMix has a spatially constant vertical temperature diffusivity equal to $10^{-5}\,m^2\,s^{-1}$, motivated by ocean interior observations. A second experiment, motivated by Munk's Abyssal Recipes and termed MunkMix, has a Munk-like vertical diffusivity of $10^{-4}\,m^2\,s^{-1}$. In the third experiment, MargMix, following Marotzke [12] and Samelson [26], κ_v is $10^{-5}\,m^2\,s^{-1}$ in the interior of the domain and $3\times10^{-3}\,m^2\,s^{-1}$ in the western and eastern boundary margins, which are each 2° in longitude and 80° in latitude (Fig. 3). The

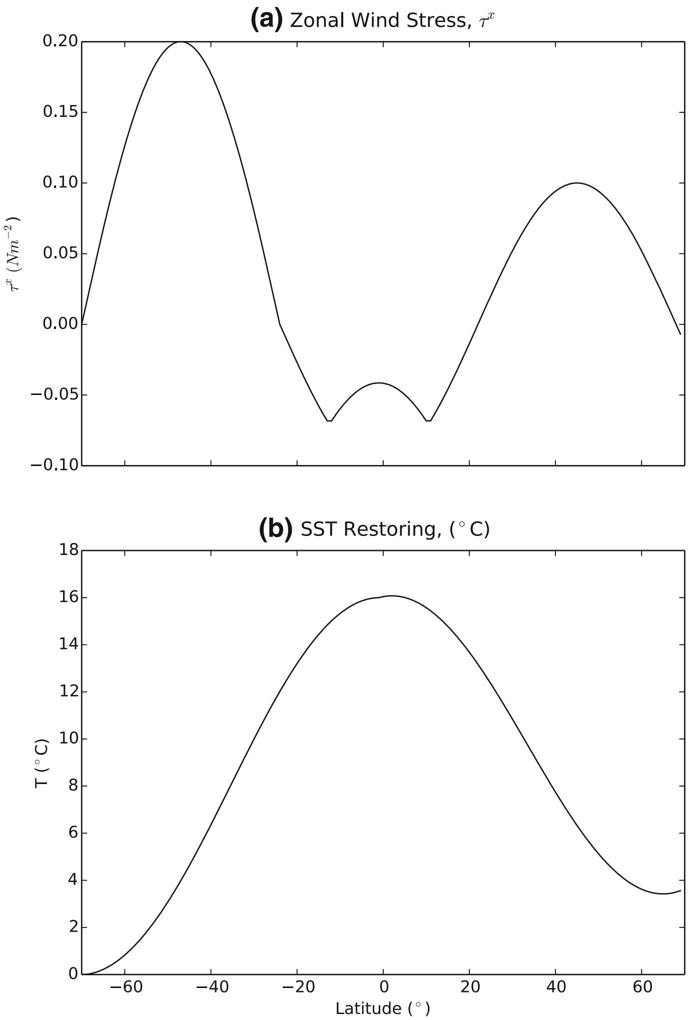

Fig. 2 Surface forcing fields for all experiments: **a** zonal wind stress, **b** SST

transition from high boundary mixing to background mixing is abrupt rather than gradual [12,26], yet a close examination of the solution shows no resulting numerical noise. The vertical diffusivity at the margins in MargMix is chosen to produce an area-average diffusivity similar to that of the MunkMix experiment. Numerical implicit diapycnal mixing is non-negligible, but its effects on stratification in our experiments are equivalent to an explicit vertical diffusivity of less than $\mathcal{O}(10^{-5})$ m^2 s^{-1}, as described in the results section below.

For averaging purposes, we define the ocean interior as the area between 40°S and 40°N. Interior zonal averages for MargMix also exclude the boundary region in which diapycnal diffusivity is elevated. The zonally integrated meridional overturning stream function, ψ, is defined as,

$$\psi(\theta, z) = -\int_{\phi_W}^{\phi_E} \int_{-H}^{z} v\, r \cos\theta \mathrm{d}z\, \mathrm{d}\phi, \tag{1}$$

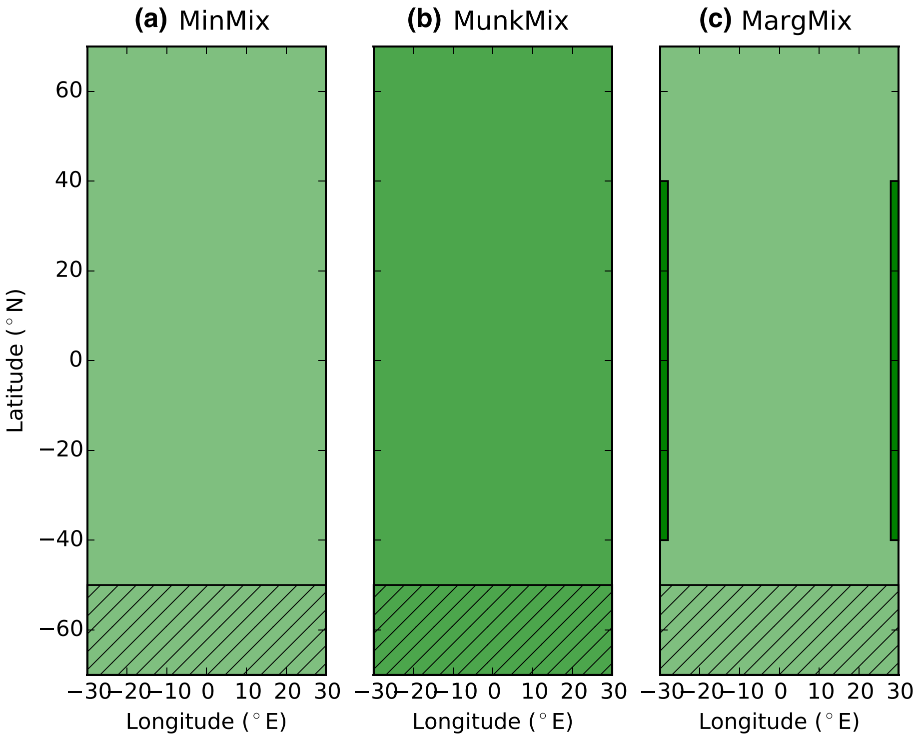

Fig. 3 Schematic of variation in background vertical diapycnal diffusivity for all experiments. Re-entrant channel is indicated by hatch marks between 70S and 50S. **a** MinMix: homogeneous low vertical mixing of 10^{-5} m^2 s^{-1}, **b** MunkMix: homogeneous higher mixing, 10^{-4} m^2 s^{-1}, **c** MargMix: low interior mixing, 10^{-5} m^2 s^{-1}, with elevated values of 3×10^{-3} m^2 s^{-1} indicated by dark green rectangles near eastern and western boundaries

where ϕ is longitude, θ is latitude, H is the bottom depth, z is the vertical coordinate, r is the radius of the Earth and v is the meridional velocity. Given the vertical velocity $w(z)$ and the diffusivity κ_v at a specific longitude and latitude, we calculate a Munk-like prediction of the temperature profile at a given horizontal location, $T_{\mathrm{Munk}}(z)$, that solves $wT_z = \kappa_v T_{zz}$. The solution is given by,

$$T_{\mathrm{Munk}}(z) = C_1 \int_{-\hat{H}}^{z} \exp\left(\int_{-\hat{H}}^{z'} \frac{w(z'')}{\kappa_v}\, \mathrm{d}z''\right) \mathrm{d}z' + C_2, \tag{2}$$

where $\hat{H} = 3000$ m (not the bottom depth of 3500 m) and the solutions are calculated only between 1000 and 3000 m depth. An optimization is used to find the integration constants C_1 and C_2 such that the solution is the best least-square fit to the model interior temperature at this location. The vertical profile $T_{\mathrm{Munk}}(z)$ is calculated separately at each horizontal location (ϕ, θ) and is then averaged horizontally. This technique is not equivalent to calculating $T_{\mathrm{Munk}}(z)$ using the ocean-average value of w due to nonlinear term in the equation for T_{Munk} involving the spatially variable w.

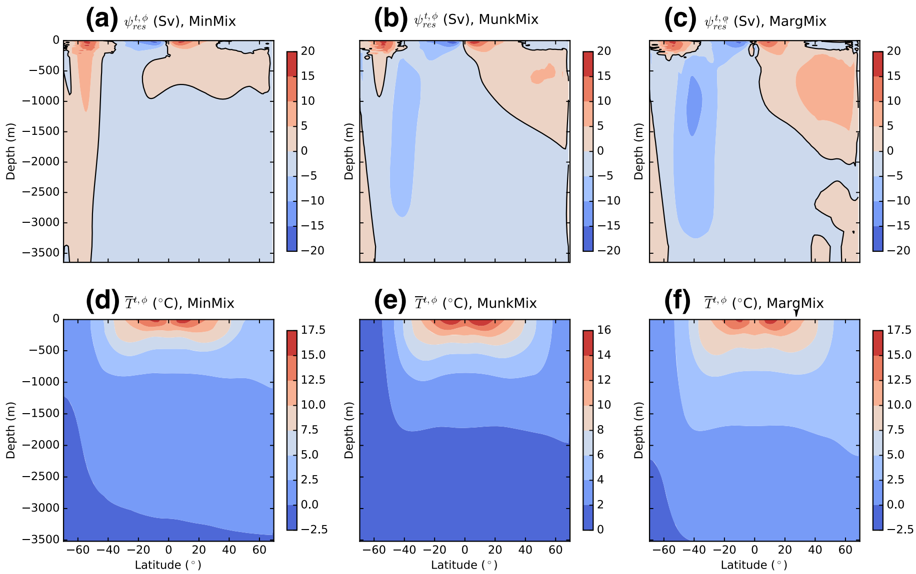

Fig. 4 Steady-state MOC residual stream function ψ_{res}, and area-weighted zonal mean T, excluding West and East boundaries, for **a**, **d** MinMix case, **b**, **e** MunkMix case, **c**, **f** MargMix case. MOC reflects Eulerian velocities plus bolus velocities calculated by the GM-Redi parameterization

3 Results

The large-scale horizontal circulation and temperature distribution in all three experiments are qualitatively similar to observed distributions (Fig. 4). The zonally averaged temperature has similar spatial structure in all cases. The surface and intermediate isopycnals outcrop in both hemispheres, and the deepest interior isopycnals outcrop in the Southern Hemisphere but not in the Northern Hemisphere. The position of the isopycnal outcrops does not vary significantly between the experiments, but the intermediate-depth stratification, which is our focus, does, as shown by the density of the isotherms in Fig. 4d–f away from the poles. The weakest interior stratification is found in the MinMix experiment, while the stratification in MunkMix and MargMix are similar.

The zonally averaged meridional residual stream function [14,38], ψ_{res}, is strongest in the MargMix experiment and weakest in the MinMax one [1,12,26]. There are clearly defined North Atlantic and Southern Ocean overturning cells in MunkMix and MargMix. The eddy-driven SO cell is opposite in sign to the Eulerian one (not shown), leading to a partial compensation, except near the surface in the SO, where the parameterization of the eddy-driven circulation breaks down due to the vertical isopycnals. The stratification differences of interest to us here appear in the zonal averages below 1000 m.

Despite large differences in the spatial structure of the diapycnal diffusivity, the interior temperature profiles for MunkMix and MargMix are almost identical, as also found by Samelson [26]. Our focus, though, is specifically the existence and mechanisms leading to an exponential profile, which he did not address. We average the intermediate-depth temperature profiles over the interior domain (40°S to 40°N and 4° inward from the eastern and western boundaries, and shown over a depth range of 1000–3000 m) and find the least-squares fit to exponential functions of the form $A + Be^{-z/h}$, where A, B and h are constants (Fig. 5). The

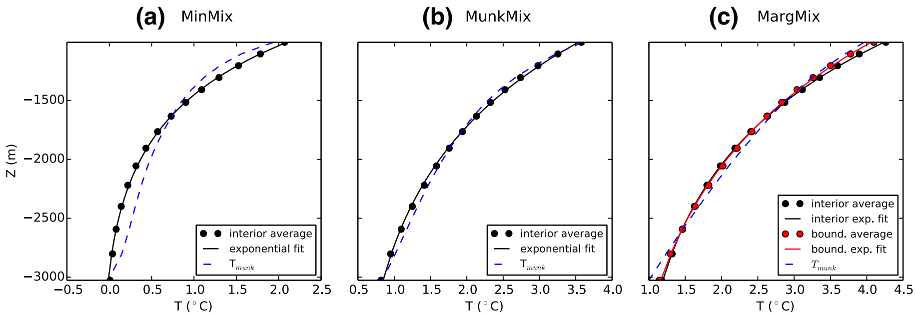

Fig. 5 Steady-state horizontally averaged temperature solution $T(z)$, $T_{\mathrm{Munk}}(z)$ solution using Eq. (2), and an exponential fit for: **a** Interior average (see Sect. 2) of MinMix solution; **b** interior average of MunkMix solution. **c** MargMix case: both interior and boundary averages calculated within 4° longitude of the West and East boundaries. $T_{\mathrm{Munk}}(z)$ is calculated and averaged in the interior for MinMix and MunkMix and averaged in the boundary region (both W and E) for the MargMix experiment. Within the respective regions, the standard deviation of $T_{\mathrm{Munk}}(z)$ is 0.1–0.3 °C

vertical decay scales, h, for the MinMix, MunkMix and MargMix cases are, respectively, 654, 1082 and 1042 m. The MunkMix and MargMix interior mid-depth stratification profiles are not only exponential but also have nearly identical vertical decay scales to each other and to the Pacific profile fitted by Munk, which had a roughly 1 km decay scale. Most importantly, all three experiments are driven by the same SO winds, yet still show differences in the mid-depth stratification, indicating that the SO does not set the mid-depth stratification by itself.

As shown in Fig. 5, the MargMix average temperature profile in the interior (where $\kappa_v = 10^{-5}\ \mathrm{m^2\ s^{-1}}$) is essentially identical to the MargMix boundary average temperature profile (where $\kappa_v = 3 \times 10^{-3}\ \mathrm{m^2\ s^{-1}}$). The boundary profile in this experiment is determined by a balance between the large upwelling and large mixing in the boundary areas, as demonstrated by the profile of $T_{\mathrm{Munk}}(z)$ computed for this experiment using Eq. (2) (dashed lines in Fig. 5). The vertical velocity in the boundary regions of MargMix is $\mathcal{O}(10^{-5})$ m/s, much larger than the interior values in all three experiments (Fig. 6). This is very different from the scenario suggested for the role of boundary mixing in the simple advection–diffusion equation of Munk and Wunsch [18], where the vertical velocity was assumed horizontally uniform.

We note that while the stratification in both MargMix and MunkMix is exponential, the vertical velocity profiles $w(z)$ are not constant in the vertical (Fig. 6). The exponential shape is thus robust, in spite of this deviation from the Munk hypothesis, as noted by Tziperman [34], see also Sect. 4 below. The exponential boundary vertical temperature profile is communicated to the interior via horizontal/isopycnal advection and mixing, consistent with the suggestion of Munk [19] and Munk and Wunsch [18], and as also found by Samelson [26] who did not address the exponential shape but just the existence of deep stratification.

The Munk balance solution (Eq. 2) for the temperature profile in MinMix is a poorer fit to the model temperature profile than it is in the MunkMix or MargMix experiments (compare dashed and solid lines in Fig. 5a, vs. b, c) because in MinMix the implicit numerical diffusivity is not negligible relative to the explicit diffusivity, $\mathcal{O}(10^{-5})\ \mathrm{m^2\ s^{-1}}$. An experiment with zero explicit vertical diffusivity yields exponential stratification with a 386 m depth, comparable to the 654 m depth scale in MinMix. Thus, because the non-negligible implicit numerical diffusivity is not accounted for in the value of κ_v used in the computation of the Munk solution, the temperature profile obtained from Eq. (2) is slightly biased. This bias due to

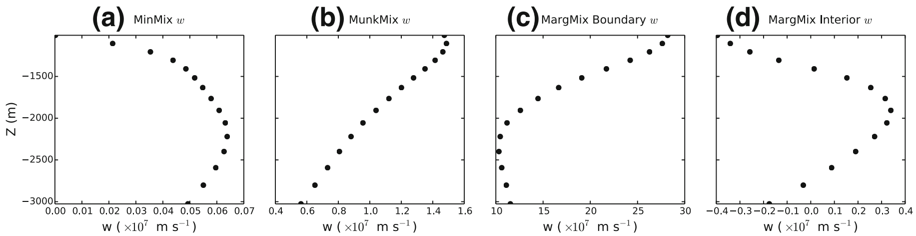

Fig. 6 Steady-state horizontally averaged $w(z)$ used to calculate T_{Munk}: **a** Interior average of MinMix solution, **b** interior average of MunkMix solution, **c** MargMix case: averaged over boundary areas

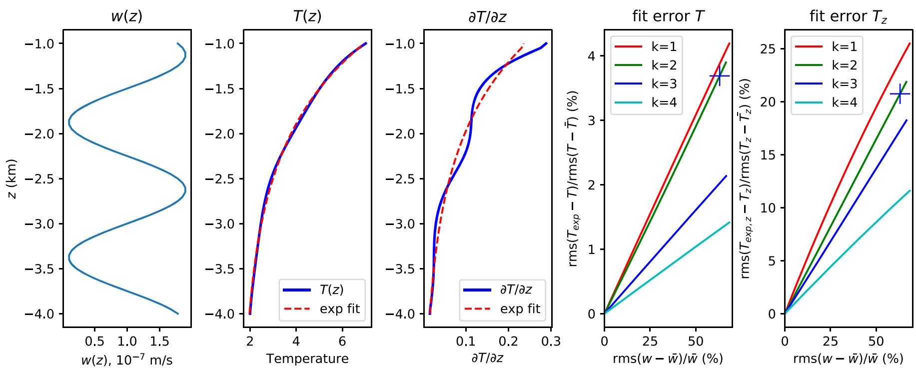

Fig. 7 Demonstrating the insensitivity of the exponential profile to variations in the vertical velocity profile. **a** A sinusoidal vertical velocity profile with wave number $k = 4$, **b** the corresponding temperature profile obtained from the Munk balance, and an exponential fit. **c** The numerical vertical derivative of the temperature profile and its exponential fit. **d**, **e** Plots of the error in fit of the temperature and its vertical derivative to exponentials, as function of the amplitude of the vertical velocity variations from the mean ($w - \overline{w}$) and for different values of the wave number, k of the imposed sinusoidal vertical velocity structure

numerical mixing is less significant in MunkMix and MargMix because the explicit vertical diffusivities are at least an order of magnitude greater than the implicit numerical diffusivity.

We also note that while the averaged vertical velocity is positive in the concentrated mixing region of MargMix as expected, it is negative in the interior of MargMix between 2500 and 3000 m (Fig. 6d), consistent with the findings of Ferrari et al. [3]. At the MargMix boundaries, the average vertical velocity is not only positive, but also three orders of magnitude greater than the MargMix interior-average vertical velocity. The sinking due to surface cooling at high latitudes is therefore balanced by lower-latitude upwelling in the margins, and the much smaller interior velocity and vertical mixing are immaterial for setting the stratification and overturning circulation in MargMix (see also [12,27]).

4 Robustness of the exponential profile

We wish to demonstrate here that if the interior (away from the SO, including boundary mixing areas) is strongly affected by diapycnal mixing, then an exponential stratification is very robust. To demonstrate this insensitivity of the exponential profile, Fig. 7a–c shows a solution to the Munk balance for a strongly varying vertical velocity and its exponential fit. We define a fit quality measure for the temperature as $\mathrm{rms}(T_{\mathrm{exp}} - T)/\mathrm{rms}(T - \bar{T})$, where

Table 1 Fit error measures between different temperature profiles shown in this paper and their exponential fits

experiment	T fit error (%)	T_z fit error (%)
MinMix	1.852	2.547
MunkMix	2.313	6.478
MargMix	1.037	12.77
W&C CP-k1	–	188.2
W&C CP-k8	–	17.66
N&V theory	–	80.88
N&V simulation	–	105.91

W&C corresponds to a calculated fit measure for the squared buoyancy frequency profile, calculated based on Fig. 13 of Wolfe and Cessi [38]; N&V similarly corresponds to Fig. 10 from Nikurashin and Vallis [22]

$T_{\rm exp}$ is the best exponential fit to the profile and $\bar{T}$ is the vertically averaged temperature. This is a non-dimensional measure of the difference between the temperature and its fit, relative to the amplitude of the vertical variations in the temperature profile itself. A similar measure is defined for the vertical derivative of the temperature profile and its best exponential fit.

These fit-quality measures are listed in Table 1 for all relevant runs in this paper, plus some from relevant previous works. The vertical velocity is assumed sinusoidal in depth with a specified amplitude and vertical wave number. Fig. 7d, e show the quality of fit as function of the amplitude of vertical velocity variation, and for different wave numbers. The amplitude of the vertical variations of the vertical velocity is measured again in nondimensional units, as $\mathrm{rms}(w - \bar{w})/\bar{w}$. This figure provides justification for the above statement [34] that the solution to the Munk balance tends to be nearly exponential even for a non-uniform vertical velocity profile. It is not surprising that the fit error is larger for the vertical derivative of the temperature, which is a more stringent measure of the quality of the exponential fit.

The error measures in the fit to an exponential profile based on the low internal diapycnal diffusivity results of Wolfe and Cessi [38] and Nikurashin and Vallis [22], which they considered their realistic regime based on the measurements of diapycnal diffusivity in the ocean interior, are listed in Table 1, and show significant deviations from an exponential profile. The high diffusivity (CP-k8, $\kappa = 0.98 \times 10^{-4}\,\mathrm{m}^2\,\mathrm{s}^{-1}$) experiment from Wolfe and Cessi [38] shows the best fit to an exponential profile, which is consistent with our MunkMix experiment results, but is less consistent with the observed low interior ocean diffusivity. These results do not contradict the role of the SO in setting a mid-depth interior stratification [5,7,21,22,35,38,39], but indicate that vertical mixing, perhaps in the boundary areas, is needed to make this interior stratification exponential.

5 Conclusions

We have examined the interaction between Southern Ocean dynamics and boundary-concentrated diapycnal mixing in the ocean interior, and demonstrated their role in setting the mid-depth (1–3 km) stratification using idealized general circulation ocean model experiments. Our focus is specifically the very robust observed exponential profile originally identified by Munk [19] and shown in Fig. 1, which was not explicitly addressed in the rich recent literature on the role of SO in setting the interior mid-depth stratification [5,21,22,35,38,39], see recent review by Johnson et al. [7]. In order to explain this exponential profile, we needed to address three challenges. First, the interior vertical diffusivity used by Munk to explain the exponential profile is much larger than that observed in the ocean interior in tracer release experiments and direct turbulence observations (Sect. 1). Second, the vertical velocity profile is not constant or spatially homogeneous as assumed by Munk. Third, recent studies have made physically convincing arguments that SO eddy dynamics must play a significant role in setting the interior (away from the SO) mid-depth stratification by communicating the surface isopycnal locations to the mid-depth interior ocean via SO isopycnal slopes set by eddy processes.

The first challenge is addressed here by examining the possibility that concentrated vertical mixing near ocean boundaries can set the stratification which is then communicated to the ocean interior by near-horizontal isopycnal eddy mixing. This possibility was already mentioned by Munk [19], and examined by later studies [12,21,26–28], although not in the context of the exponential mid-depth stratification. Munk and Wunsch [18] did examine the effect of boundary mixing on the interior exponential stratification using a simple advection–diffusion model. They *assumed* that the vertical velocity is horizontally uniform and showed how boundary mixing leads to exponential interior stratification in the limit of infinitely efficient horizontal spreading. We find a very different picture in the concentrated mixing areas at the ocean margins, where both the vertical velocity and vertical mixing are orders of magnitude larger than those in the ocean interior away from horizontal boundaries. The ratio of vertical velocity and mixing rate in the boundary areas still yields an $\mathcal{O}(1000)$ m depth scale, similar to that of the observed interior stratification profile. The vertical stratification profile and exponential scale are therefore nearly identical to those we find with a uniform Munk-like vertical mixing throughout the ocean interior. We also find that even in the presence of a SO-like channel, an exponential stratification with an observed-like depth scale cannot develop with a weak or vanishing diapycnal mixing. Ferrari et al. [3], who studied the role of sloping ocean boundaries, also found strong upwelling near the (sloping) boundaries and downwelling in the interior, although they did not explicitly address the issue of exponential stratification.

As for the second challenge, we demonstrated in Sect. 4 that the solution to the Munk balance of $w\rho_z = \kappa_v \rho_{zz}$ is very closely exponential even when the vertical velocity is specified to vary fairly strongly in the vertical direction (see also [34]). This robustness of the exponential profile was also demonstrated in the concentrated boundary mixing regions of our idealized GCM experiments, where the vertical velocity is both very large and strongly varying in depth. The existence of an exponential profile at a depth as shallow as 1 km [19] together with our results here suggest that diapycnal mixing is likely a strong player even at this density range. The strong mixing limit of Nikurashin and Vallis [21,22] was suggested as being relevant to the abyssal ocean, and while these works did not address the exponential stratification profile, we add here that such a strong vertical mixing limit may be relevant in the mid-depth ocean as well, via the action of boundary mixing.

These results are consistent with the hypothesis that the mid-depth stratification is determined by the condition that the net mass flux across any isopycnal surface must vanish at a steady state, used by Tziperman [34] to calculate the basic stratification of both the mid-depth ocean and of inviscid upper ocean thermocline theories that needed to specify the basic eastern boundary stratification [11,25]. Cooling at the surface of the SO near some isopycnal ρ_1, for example, leads to a water-mass transformation across this isopycnal and toward higher densities [30,34,36]. This flux must be balanced by upward cross-isopycnal mass flux in the ocean interior toward density ranges lighter than ρ_1. The interior fluxes are driven by small-scale mixing which depends on the vertical stratification there. If the surface cross-isopycnal flux is larger than the interior one, this leads to accumulation of water mass in the deep ocean below the density ρ_1, adjusting the mid-depth stratification. This change in mid-depth stratification would drive an adjustment in gradient-driven interior diapycnal mass fluxes and possibly also change the surface outcrop location of ρ_1 and therefore the air sea fluxes and the surface transformation across this isopycnal. Thus the outcrop positions and deep stratification must co-evolve until a zero net flux across each isopycnal is achieved and an equilibrium is reached [34]. The deep stratification set by this balance is exponential because, as was explained above, the solution of $w(z)\rho_z = (\kappa(z)\rho_z)_z$ is very nearly exponential even if the upwelling or diffusivity are not constant in z. In the picture presented here, the eddies setting the SO isopycnal slopes play an important role in communicating between surface density gradients in the SO (and in the North Atlantic, in the more realistic scenario [38,39]) and establishing a basic mid-depth stratification [5,7,21,22,35,38,39]. Diapycnal boundary mixing can then act to adjust this mid-depth stratification to result in an exponential profile. All three processes—SO eddies, surface water mass transformation, and interior diapycnal mixing—must be playing a role in setting the exponential mid-depth stratification.

There are numerous idealizations used here, and many quantitative issues regarding the role of boundary mixing that should be further explored with closer examination of observations. For example, we do not address the observation that the deep ocean under the main thermocline includes both isopycnals that outcrop in the SO and those that outcrop in the North Atlantic, leading to possibly different dynamics [38]. Our simulation domain are idealized, eddies are not resolved, the effects of salinity are ignored, the specified boundary mixing is crude, and more. We also did not include the effects of sloping boundaries, which was suggested to play an important role in Ferrari et al. [3]. Similarly, we do not discuss the effect of vertical variations in the vertical mixing coefficient that was suggested by Mashayek et al. [16]. This study focused on the deep and bottom layers underneath what the first group of studies mentioned in the introduction considered the "adiabatic layer". It showed that when the vertical mixing is enhanced near the bottom and decays upward, the stratification is nearly exponential in their deep layer (1.5–3 km depth), where the balance is indeed the Munk balance (their equation 14). Mashayek et al. [16] did not explicitly address the issue of an exponential stratification with an *observed-like* scale in depth ranges where one expects to see smaller vertical diffusion (one expects numerical diffusion to be significant in their coarse resolution model, as found in our similarly coarse simulations). They also did not address the question of an exponential stratification when the vertical velocity is not uniform, but they did present an alternative to the boundary mixing scenario considered here.

The current study should therefore be viewed merely as an idealized exploration of processes that can lead to a mid-depth exponential stratification with an observed-like vertical scale, rather than a quantitative or definite explanation of the observed stratification.

Acknowledgements MDM and ET were supported by NASA ROSES Grant NNX14AH39G and NSF Physical Oceanography Grant OCE-1535800. XY was supported by a summer undergraduate research fellowship from Peking University. Computational resources were provided by the NASA High-End Computing (HEC) Program through the NASA Advanced Supercomputing Center at NASA Ames and the NASA Center for Climate Simulation (NCCS) at Goddard Space Flight Center and on the Odyssey cluster supported by the FAS Division of Science, Research Computing Group at Harvard University. ET thanks the Weizmann Institute for its hospitality during parts of this work. All data and programs used for this study are available from the corresponding author.

References

1. F. Bryan, Parameter sensitivity of primitive equation ocean general circulation models. J. Phys. Oceanogr. **17**, 970–985 (1987)
2. K. Bryan, Accelerating the convergence to equilibrium of ocean-climate models. J. Phys. Oceanogr. **14**, 666–673 (1984)
3. R. Ferrari, A. Mashayek, T.J. McDougall, M. Nikurashin, J.-M. Campin, Turning ocean mixing upside down. J. Phys. Oceanogr. **46**(7), 2239–2261 (2016)
4. P.R. Gent, J. Willebrand, T.J. Mcdougall, J.C. Mcwilliams, Parameterizing eddy-induced tracer transports in ocean circulation models. J. Phys. Oceanogr. **25**(4), 463–474 (1995)
5. C.C. Henning, G.K. Vallis, The effects of mesoscale eddies on the stratification and transport of an ocean with a circumpolar channel. J. Phys. Oceanogr. **35**(5), 880–896 (2005)
6. T. Ito, J. Marshall, Control of lower-limb overturning circulation in the Southern Ocean by diapycnal mixing and mesoscale eddy transfer. J. Phys. Oceanogr. **38**(12), 2832–2845 (2008)
7. H.L. Johnson, P. Cessi, D.P. Marshall, F. Schloesser, M.A. Spall, Recent contributions of theory to our understanding of the Atlantic meridional overturning circulation. J. Geophys. Res. Oceans **124**(8), 5376–5399 (2019)
8. W.G. Large, J.C. Mcwilliams, S.C. Doney, Oceanic vertical mixing: a review and a model with a nonlocal boundary-layer parameterization. Rev. Geophys. **32**(4), 363–403 (1994)
9. J.R. Ledwell, A.J. Watson, C.S. Law, Mixing of a tracer in the pycnocline. J. Geophys. Res. **103**(C10), 21499–21529 (1998)
10. R. Lumpkin, K. Speer, Global ocean meridional overturning. J. Phys. Oceanogr. **37**, 2550–2562 (2007)
11. J.R. Luyten, J. Pedlosky, H. Stommel, The ventilated thermocline. J. Phys. Oceanogr. **13**(2), 292–309 (1983)
12. J. Marotzke, Boundary mixing and the dynamics of three-dimensional thermohaline circulations. J. Phys. Oceanogr. **27**(8), 1713–1728 (1997)
13. J. Marshall, A. Adcroft, C. Hill, L. Perelman, C. Heisey, A finite-volume, incompressible Navier–Stokes model for studies of the ocean on parallel computers. J. Geophys. Res. **102**, 5753–5766 (1997)
14. J. Marshall, T. Radko, Residual-mean solutions for the Antarctic Circumpolar Current and its associated overturning circulation. J. Phys. Oceanogr. **33**(11), 2341–2354 (2003)
15. J. Marshall, T. Radko, A model of the upper branch of the meridional overturning of the Southern Ocean. Progr. Oceanogr. **70**(2), 331–345 (2006)
16. A. Mashayek, R. Ferrari, M. Nikurashin, W.R. Peltier, Influence of enhanced abyssal diapycnal mixing on stratification and overturning circulation. J. Phys. Oceanogr. **45**, 2580–2597 (2015)
17. A. Melet, R. Hallberg, S. Legg, K. Polzin, Sensitivity of the ocean state to the vertical distribution of internal-tide driven mixing. J. Phys. Oceanogr. **43**, 602–615 (2013)
18. W. Munk, C. Wunsch, Abyssal recipes II: energetics of tidal and wind mixing. Deep-Sea Res. Part I-Oceanogr. Res. Pap. **45**(12), 1977–2010 (1998)
19. W.H. Munk, Abyssal recipes. Deep Sea Res. Oceanogr. Abstr. **13**(4), 707–730 (1966)
20. J.D. Nash, S.M. Kelly, E.L. Shroyer, J.N. Moum, T.F. Duda, The unpredictable nature of internal tides on continental shelves. J. Phys. Oceanogr. **42**, 1981–2000 (2012)
21. M. Nikurashin, G. Vallis, A theory of deep stratification and overturning circulation in the ocean. J. Phys. Oceanogr. **41**(3), 485–502 (2011)
22. M. Nikurashin, G. Vallis, A theory of the interhemispheric meridional overturning circulation and associated stratification. J. Phys. Oceanogr. **42**, 1652–1667 (2012)
23. K.L. Polzin, J.M. Toole, J. Ledwell, R.W. Schmitt, Spatial variability of turbulent mixing in the abyssal ocean. Science **276**(5309), 93–96 (1997)
24. M.H. Redi, Oceanic isopycnal mixing by coordinate rotation. J. Phys. Oceanogr. **12**, 1154–1158 (1982)
25. P.B. Rhines, W.R. Young, A theory of the wind-driven circulation. I. Mid-ocean gyres. J. Mar. Res. **40**(3), 559–596 (1982)
26. R. Samelson, Large-scale circulation with locally enhanced vertical mixing. J. Phys. Oceanogr. **28**(4), 712–726 (1998)
27. J.R. Scott, J. Marotzke, The location of diapycnal mixing and the meridional overturning circulation. J. Phys. Oceanogr. **32**(12), 3578–3595 (2002)
28. C.J. Shakespeare, A. McC, Hogg, An analytical model of the response of the meridional overturning circulation to changes in wind and buoyancy forcing. J. Phys. Oceanogr. **42**(8), 1270–1287 (2012)
29. K.L. Sheen, J.A. Brearley, A.C. Naveira Garabato, D.A. Smeed, S. Waterman, J.R. Ledwell, M.P. Meredith, L. St. Laurent, A.M. Thurnherr, J.M. Toole et al., Rates and mechanisms of turbulent dissipation and mixing in the Southern Ocean: results from the diapycnal and isopycnal mixing experiment in the Southern Ocean (DIMES). J. Geophys. Res. Oceans **118**(6), 2774–2792 (2013)

30. K. Speer, E. Tziperman, Rates of water mass formation in the North-Atlantic Ocean. J. Phys. Oceanogr. **22**(1), 93–104 (1992)
31. L. St. Laurent, A.C. Naveira Garabato, J.R. Ledwell, A.M. Thurnherr, J.M. Toole, A.J. Watson, Turbulence and diapycnal mixing in Drake Passage. J. Phys. Oceanogr. **42**(12), 2143–2152 (2012)
32. L.C. St. Laurent, A.M. Thurnherr, Intense mixing of lower thermocline water on the crest of the Mid-Atlantic Ridge. Nature **448**(7154), 680–683 (2007)
33. AM. Thurnherr, L. St. Laurent, Turbulence and diapycnal mixing over the East Pacific Rise crest near 10°N. Geophys. Res. Lett. **38**, L15613 (2011)
34. E. Tziperman, On the role of interior mixing and air-sea fluxes in determining the stratification and circulation of the oceans. J. Phys. Oceanogr. **16**, 680–693 (1986)
35. G.K. Vallis, Large-scale circulation and production of stratification: effects of wind, geometry, and diffusion. J. Phys. Oceanogr. **30**(5), 933–954 (2000)
36. G. Walin, On the relation between sea-surface heat flow and the thermal circulation in the ocean. Tellus **34**, 187–195 (1982)
37. A.F. Waterhouse et al., Global patterns of diapycnal mixing from measurements of the turbulent dissipation rate. J. Phys. Oceanogr. **44**, 1854–1872 (2014)
38. C.L. Wolfe, P. Cessi, What sets the strength of the middepth stratification and overturning circulation in eddying ocean models? J. Phys. Oceanogr. **40**, 1520–1538 (2010)
39. C.L. Wolfe, P. Cessi, The adiabatic pole-to-pole overturning circulation. J. Phys. Oceanogr. **41**(9), 1795–1810 (2011)